Thermochimica Acta, 91 (1985) 311–320
Elsevier Science Publishers B.V., Amsterdam – Printed in The Netherlands

THERMOGENESIS: AN APPLICATION TO THE MARTENSITIC TRANSFORMATION: ENTROPY, ENTHALPY AND ACOUSTIC EMISSION FOR A Cu–Al–Mn–Fe ALLOY

C. PICORNELL, C. SEGUI and V. TORRA

Departament de Fisica, Facultat de Ciències, Universitat de Palma de Mallorca, 07071 Palma de Mallorca (Spain)

J. HERNAEZ and C. LOPEZ DEL CASTILLO

Departamento de Metalurgia, Facultad de Quimica, Universitad Complutense, 28071 Madrid (Spain)

(Received 30 March 1985)

ABSTRACT

An experimental set-up, designed for the simultaneous measurement of the thermal energy and the acoustic emission produced by a solid–solid martensitic transformation, is described. Different polycrystalline samples of a Cu–Al–Mn–Fe alloy have been studied with this system after different thermal treatments. For an aged sample, the following values have been obtained: $M_s = 10$, $M_f = -32$, $A_s = 5$ and $A_f = 37$°C, and $\Delta S = 0.028$ J K^{-1} g^{-1}, $\Delta H = 7.50$ J g^{-1}. The acoustic emission produced during the transformation and the thermal energy rate obtained from the calorimetric response by means of a deconvolution procedure show strong correlation. Within the experimental performances the transformation shows a discontinuous character.

INTRODUCTION

Martensitic transformations are first-order solid–solid transitions between metastable phases. In certain copper-based alloys, the high-temperature β-phase transforms, on cooling, to a martensitic phase. The transformation being reversible, completion of the cycle by heating restores the β-phase. By means, on one side, of highly sensitive microcalorimeters (using semiconductive thermocouples) at slow temperature programs and, on the other side, of the appropriate methods of signal treatment, it has been possible to show important discontinuous components in the transformation.

Particularly, concerning Cu–Zn–Al alloys, coupled measurements have been performed of the calorimetric response and acoustic emission during the martensitic transformation [1]. In part of these experiments, the change in electrical resistivity of the sample has also been determined simultaneously [2].

In this work, together with the basic characteristics of the alloy and the corresponding heat treatments performed on the samples under study, we describe an experimental system designed for

(1) evaluation of the enthalpy and entropy changes during the transformation,

(2) determination of the characteristic temperatures corresponding to the beginning (s = start) or to the end (f = finish) of the direct and reverse transformation, namely M_s, M_f, A_s and A_f,

(3) recording of the acoustic emission.

Several experiments with extremely low heating and cooling rates (~ 0.01 K min^{-1}) have also been carried out. They have shown the essentially discontinuous character of the transformation for both the release of thermal power and the acoustic emission.

PREPARATION, MICROSTRUCTURAL CHARACTERIZATION AND HEAT TREATMENTS OF THE SAMPLES

The polycrystalline alloy, with mean composition 81.2 Cu, 11.8 Al, 6.8 Mn, 0.2 Fe (wt%), was obtained by melting components with a purity degree higher than 99.8% in a high-frequency induction furnace with an argon controlled atmosphere. Two sequential meltings were carried out prior to the final casting.

Finally, the "as-casted" material was annealed for 25 h at 800°C, 24 h at 750°C and water-quenched to room temperature. Prismatic samples (6.45 × 8.20 × 2.86 mm) were obtained by mechanical cutting from the ingot and

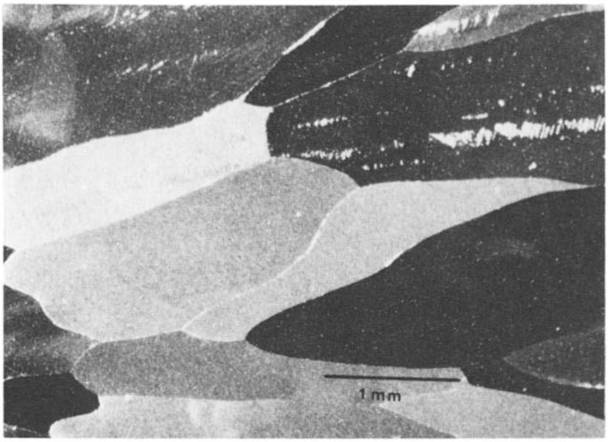

Fig. 1. Macrography of the sample showing the lenticular microstructure and the grain size.

aged at room temperature for one year. The chemical composition of the alloy was determined by atomic absorption.

The metallographic characterization, after electrolytic polishing and etching, revealed a polycrystalline microstructure with lenticular morphology and mean grain size of 0.95 mm (Fig. 1; sample named BHT).

After thermal cycling, the sample under study was thermally treated again at 800°C for 2 h, and immediately quenched in water at 20°C. A new metallographic observation shows the same morphology with a slightly bigger grain size of 1.01 mm (sample named AHT). The composition also slightly varies, the change in Fe being relatively the more important (from 0.2 to 0.4 wt%).

EXPERIMENTAL SET-UP

The sample under study and the thermal and acoustic transducers are placed upon a central slider, as shown in Fig. 2. The whole calorimeter is built from copper. The main time constant in our working conditions centres around 12 s; it changes with temperature, and the whole relative variation in the working temperature domain is of the order of 40%. The sensibility of the device also varies with temperature, from 50 mV/W for the lowest temperatures to 300 mV/W for the highest ones [3].

The temperature of the calorimetric block is measured by means of a Pt-resistance probe with a resolution of 0.01°. The effective working interval ranges between 80 and 380 K. The temperature programs can be adjusted between 0.01 and 0.5 K min^{-1}.

The thermal signal is detected by means of two semiconducting thermoelectric batteries (Melcor FC 0.6.66-05L) connected in differential and placed on both sides of the central slider. One of them is in direct contact

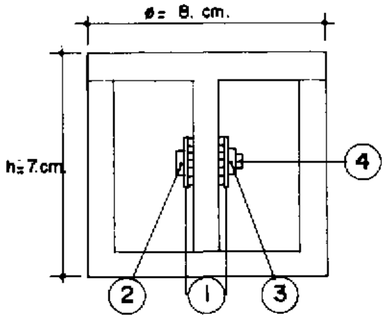

Fig. 2. Vertical section of the calorimeter: (1) thermocouples, (2) reference sample, (3) sample, (4) acoustic detector.

with the sample, and the other is in contact with a brass reference of similar mass and geometry. The signal is digitized by means of a digital voltmeter (Datron DC 1055; resolution 100 nV) and stored on a floppy disk. Two different types of measurements have been carried out, namely:

(A) slow data acquisition in which every recorded point is an average of several output data, giving, in this way, an integrated description of the whole transformation. The sampling period for every recorded datum is around 2.5 s;

(B) fast data acquisition, with blocks consisting of 7000 points and one point sampled each 0.08 s. This enables the detailed study of partial intervals in the transformation.

The thermogram can be numerically treated to partially eliminate the thermal inertia of the calorimeter. The results of deconvolution give a good picture of the thermal kinetics of the transformation [4].

The acoustic signal is detected by means of a piezoelectric transducer (Philips PXE 5) attached to the top surface of the sample. It is conveniently amplified and filtered (preamplifier Bruel and Kjaer 2637 with gain of 40 dB, and amplifier Bruel and Kjaer 2638 with adjustable gain between 0 and 60 dB and frequency bandwidth ranging from 200 KHz to 2 MHz) and, after rectification, it is analysed and stored in the memory of a Canberra Series 35 multichannel analyser (1024 channels). Two analyses can be performed: either the rate of the number of counts above a certain threshold as a function of time, $\dot{N}(t)$, together with the accummulated number of counts, $N(t)$, or the amplitude distribution of the acoustic events. From the amplitude distribution, the mean energy, E, of the acoustic activity in the time interval (t_1, t_2) can be computed from the expression

$$E(t_1, t_2) \approx \Sigma N_i i^2$$

where N_i is the number of events accumulated in the i-th channel [5].

Figure 3 shows a block diagram representing the experimental set-up designed for the acquisition and storage of the acoustic and thermal signals generated during the martensitic transformation.

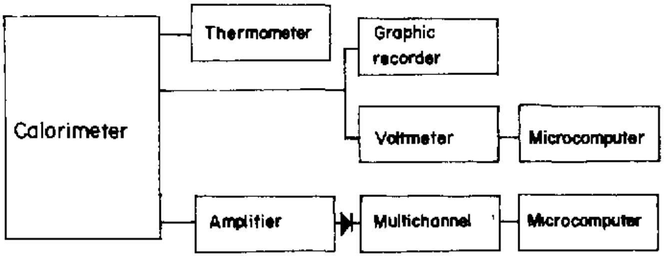

Fig. 3. Block diagram for the experimental system and the data acquisition chain.

RESULTS

Before any systematic treatment of the Cu–Al–Mn–Fe alloy, a preliminary study was carried out in order to estimate the temperature range and the values of enthalpies and entropies for both the forward and reverse transformations. This consisted of eleven thermal cycles performed on a sample from the same cast, with the same nominal composition and after a heat treatment analogous to that of the sample BHT [6].

The systematic study was then carried out. Eleven heating and cooling cycles were performed in the temperature range 70 to −60°C, ten of them with temperature programmes between 0.1 and 0.3 K min^{-1} and the eleventh one with a very slow temperature programme (~ 0.01 K min^{-1}). After the annealing heat treatment, the first ten thermal cycles with fast temperature programmes were again performed.

Table 1 shows for a few cycles, either before or after the heat treatment, the temperatures at which the direct and reverse transformations begin or finish, as pointed out by the first or last signal of thermal activity from the calorimeter. The temperatures corresponding to 10 and 90% of the total energy released are also given. It can be noticed that M_f and A_s for corresponding cycles before and after the thermal treatment remain almost unchanged, while M_s and A_f shift to higher temperatures. However, the differences $(A_s - M_f)$ or $(A_f - M_s)$, and in this sense the transformation hysteresis, remain practically constant. This observation is coherent with the constancy of the transformation hysteresis between aged and quenched β-CuZnAl alloys [7]. The shift in the M_s temperature can be partially related to quenching and to change in composition after the heat treatment of the sample AHT. In Fig. 4, corresponding to the tenth cycle, the shift in M_s and A_f can be seen for the accumulated enthalpy.

TABLE 1

Temperatures M_s, M_f, A_s and A_f at which the direct and reverse transformations begin or finish, together with the temperatures M_s*, M_f*, A_s* and A_f* corresponding to 10 and 90% of the total energy dissipation in both transformations. The symbol BHT corresponds to cycles before the annealing thermal treatment, and AHT to those after it. All the temperatures are given in °C

Cycle No.	3 BHT	10 BHT	3 AHT	10 AHT
M_s	10	14	26	28
M_f	−32	−32	−33	−32
A_s	6	5	3	2
A_f	37	35	53	53
M_s*	−4	−4	1	−1
M_f*	−20	−22	−21	−21
A_s*	11	9	8	8
A_f*	23	21	26	26

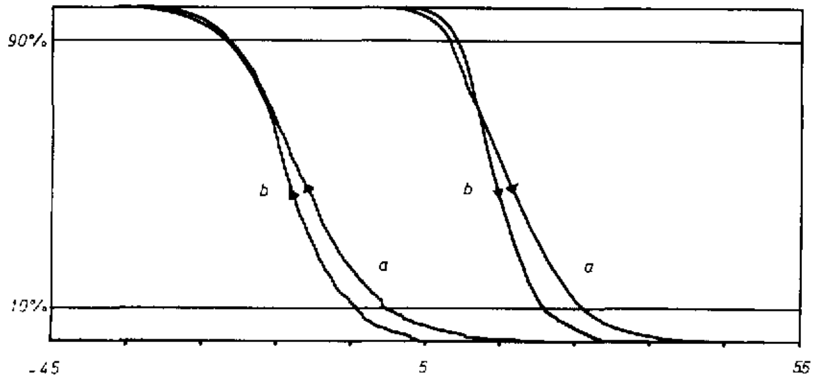

Fig. 4. Thermal power integrated as a function of temperature for the tenth cycle, before (b) and after (a) the annealing heat treatment. The graph being normalized to the total energy, the relative location of the temperatures corresponding to 10 and 90% of total thermal activity is also shown.

Table 2 presents the results for the total changes in enthalpy and entropy obtained from numerical integration of the thermogram taking into account the dependence of both the sensibility on temperature and the temperature on time [3].

Concerning acoustic activity, Table 3 shows the results for the first and tenth cycles before and after the thermal treatment. The acoustic activity decreases by a factor of two from one cycle to the other, independently of the heat treatment. Both the mean acoustic energy and the total number of counts are clearly larger for the reverse than for the direct transformation. This fact has already been mentioned in the literature for copper-based memory alloys [8,9]. Our calculations show, however, that the mean acoustic energy per ringdown count, E/N, is not a constant, but is approximately double on heating than on cooling.

Figure 5 shows the characteristic thermograms of the direct and reverse transformations together with either the accumulated number of counts or the accumulated acoustic energy as a function of temperature.

The instantaneous thermal power computed from the experimental thermogram is shown in Fig. 6 together with the rate of acoustic ringdown

TABLE 2

Values for the enthalpy changes, $\Delta H^{\beta \to M}$ and $\Delta H^{M \to \beta}$ (J g^{-1}), and for the entropy changes, $\Delta S^{\beta \to M}$ and $\Delta S^{M \to \beta}$ (J K^{-1} g^{-1}), for the direct and reverse transformations

Cycle No.	3 BHT	10 BHT	3 AHT	10 AHT
$\Delta H^{\beta \to M}$	−7.22	−7.51	−8.00	−7.71
$\Delta H^{M \to \beta}$	7.13	7.35	8.18	8.25
$\Delta S^{\beta \to M}$	−0.028	−0.029	−0.030	−0.029
$\Delta S^{M \to \beta}$	0.025	0.025	0.028	0.028

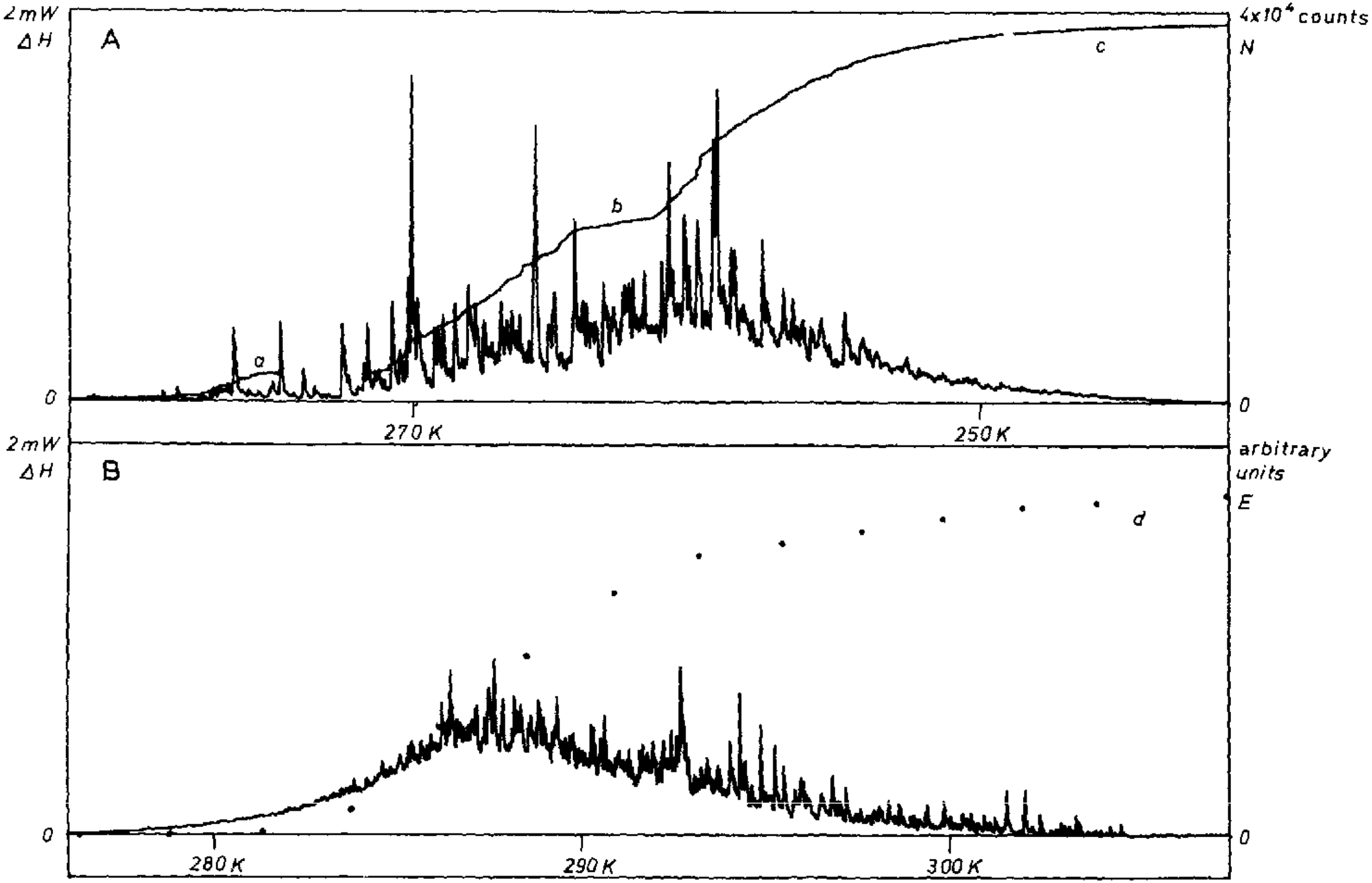

Fig. 5. (A) Characteristic thermogram in a measurement of the energy released during the transformation $\beta \rightarrow$ M. The sampling period is $\Delta t = 2.45$ s and the cooling rate is $\mathrm{d}T/\mathrm{d}t \approx -0.26$ K min^{-1}. The accumulated number of counts, $N(T)$, is also shown as a function of temperature (lines a, b, c). (B) Characteristic thermogram for the energy released during the reverse transformation M $\rightarrow \beta$, with a sampling period $\Delta t = 2.42$ s and a heating rate $\mathrm{d}T/\mathrm{d}t \approx 0.17$ K min^{-1}, together with the accumulated acoustic energy, E, as a function of the temperature (curve d).

counts, for a limited interval of temperatures of the direct transformation, showing a good correspondence between the two signals. In the same figure, part of a reverse transformation carried out with a very low heating rate is also shown, As the transformation proceeds very slowly, it appears to be of discontinuous character and, in this sense, the idea of a low, continuous background overlapped with several sudden, sharp peaks should be discarded.

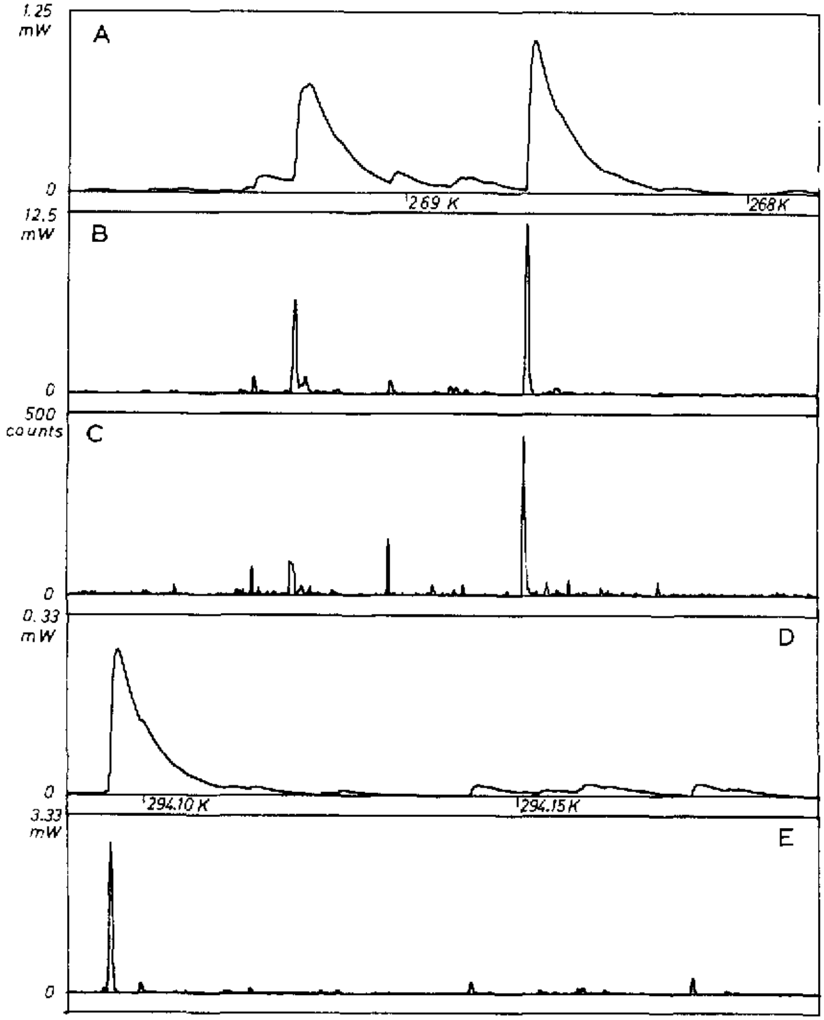

Fig. 6. (A) Kinetic study of a limited interval in the transformation $\beta \rightarrow$ M. The thermogram is sampled each $\Delta t = 0.086$ s and the rate of change in temperature is $dT/dt \approx -0.22$ K min^{-1}. (B) Deconvolution of the preceding thermogram, giving the instantaneous thermal power released as a function of temperature. (C) The corresponding acoustic emission. (D) Thermogram for a local study of the transformation M $\rightarrow \beta$, with a sampling period $\Delta t = 0.085$ s and a heating rate $dT/dt \approx 0.01$ K min^{-1}. (E) Deconvolution of the preceding thermogram.

TABLE 3

Total number of ringdown counts, N, total acoustic energy, E, and mean acoustic energy per count, $\langle E \rangle = E/N$, for different corresponding cycles before or after the annealing treatment. E and $\langle E \rangle$ are given in arbitrary units

Cycle No.	1 BHT	10 BHT	1 AHT	10 AHT
Direct transformation				
N	37800	26960	31270	14220
E	0.233	0.172	0.297	0.122
$\langle E \rangle$	0.616	0.638	0.950	0.858
Reverse transformation				
N	131390	69020	120840	51270
E	1.746	0.944	1.984	0.711
$\langle E \rangle$	1.329	1.368	1.642	1.387

CONCLUSIONS

(1) An austenitic Cu–Al–Mn–Fe alloy, with nominal composition (wt%): 11.79 Al, 6.80 Mn, 0.17 Fe, transforms martensitically with characteristic temperatures: $M_s = 10$, $M_f = -32$, $A_s = 5$ and $A_f = 37°\text{C}$. After an annealing heat treatment, M_f and A_s remain practically unchanged whereas M_s and A_f shift to higher temperatures. The changes in entropy and enthalpy amount (on average) to $\Delta S = 0.028$ J K^{-1} g^{-1} and $\Delta H = 7.50$ J g^{-1}.

(2) The acoustic activity, namely the total number of ringdown counts and the mean acoustic energy, decreases with the number of cycles. It is always higher for the reverse transformation than for the direct one. The mean acoustic energy per count is stable with the number of cycles but it is roughly double on heating than on cooling.

(3) Deconvolution of the thermograms enables comparison between the energy dissipation and the acoustic emission, showing a remarkable correspondence in time. Very slow cooling and heating rates (~ 0.01 K min^{-1}) clearly show a discontinuous behaviour of the transformation. In the frame of the actual experimental conditions the thermal and acoustic kinetics of the transformation do not have continuous components.

ACKNOWLEDGEMENTS

The present work is part of a more extensive research program in materials science carried out by the Universities of Palma, Barcelona and Madrid. Materials research at the University of Palma de Mallorca is supported by a grant of the CAICYT (Spain). The authors gratefully acknowledge Prof. J.M. Guilemany, University of Barcelona, and Dr. J.

Ortin, University of Palma de Mallorca, for their clarifying contributions. One of the authors (C.S.) also acknowledges a fellowship from the "Ministerio de Educacion y Ciencia" within the "Plan Nacional de Formacion de Personal Investigador". (CAICyT number 3562-83.)

REFERENCES

1 A. Planes, J.L. Macqueron, M. Morin and G. Guenin, Phys. Status Solidi A, 66 (1981) 717.
2 J.L Macqueron and M. Robin, Proc. Jornades de Transformacions Termoelastiques, Palma de Mallorca, 1984, pp. E01–E13.
3 J.P. Dubes, H. Tachoire, J.L. Macqueron, J. Ortin, C. Picornell, C. Segui and V. Torra, Proc. Jornades de Transformacions Termoelastiques, Palma de Mallorca, 1984, pp. h01–h07.
4 E. Cesari, A. Planes, V. Torra, J.L. Macqueron and J.P. Dubes, Bull. Soc. Chim. Fr., (1983) I-89.
5 J. Baram, J. Avissar, Y. Gefen and M. Rosen, Scr. Metall., 14 (1980) 1013.
6 J. Hernaez, C. Lopez del Castillo, J. Ortin, C. Picornell, C. Segui and V. Torra, Proc. Jornades de Transformacions Termoelastiques, Palma de Mallorca, 1984, pp. c01–c13.
7 R. Rapacioli and M. Ahlers, Acta Metall., 27 (1979) 777.
8 A. Planes, D. Rouby, J.L. Macqueron, M. Morin and G. Guenin, J. Phys. D.: Appl. Phys., 15 (1982) 89.
9 D. Maeder, P. Ryser, D. Sanderson, A. Sillou and A. Steiner, Acta Metall., 31 (1983) 2113.